Acta Crystallographica Section D
Biological Crystallography
ISSN 0907-4449

Different orientations of low-molecular-weight fragments in the binding pocket of a BRD4 bromodomain

Graziano Lolli[a,b]* and Roberto Battistutta[a,b]

[a]Department of Chemical Sciences, University of Padova, Via Marzolo 1, 35131 Padova, Italy, and [b]Venetian Institute of Molecular Medicine, Via Orus 2, 35129 Padova, Italy

Correspondence e-mail: graziano.lolli@unipd.it

Received 11 January 2013
Accepted 19 July 2013

PDB References: N-terminal bromodomain of BRD4, complex with *N*-methyltrimethylacetamide, 4ioo; complex with pyrrolidin-2-one, 4ioq; complex with DMSO, 4ior

Bromodomains are involved in the regulation of chromatin architecture and transcription through the recognition of acetylated lysines in histones and other proteins. Many of them are considered to be relevant pharmacological targets for different pathologies. Three crystallographic structures of the N-terminal bromodomain of BRD4 in complex with low-molecular-weight fragments are presented. They show that similar molecules mimicking acetylated lysine bind the bromodomain with different orientations and exploit different interactions. It is also advised to avoid DMSO when searching for low-affinity fragments that interact with bromodomains since DMSO binds in the acetylated lysine-recognition pocket of BRD4.

1. Introduction

Bromodomains (BRDs) are protein modules that recognize acetylated lysines (K_{ac}) in histones and other proteins. BRDs are present in diverse proteins including acetylases, helicases, methyltransferases, transcriptional mediators and the bromo and extra-terminal (BET) family (Filippakopoulos, Picaud, Mangos *et al.*, 2012), covering important roles in the regulation of chromatin architecture and transcription. All BRDs have a common left-handed helical bundle fold with four antiparallel helices (αZ, αA, αB and αC) connected by the two ZA and BC loops. K_{ac} binds in a deep central hydrophobic cavity, anchoring to an asparagine residue present in most BRDs by a hydrogen bond (Owen *et al.*, 2000).

Several reports encourage the development of BRD inhibitors for therapeutic purposes. Restricting the field to BRD4, a member of the BET family, many studies have identified this protein as a valuable target in cancer. It directs post-mitotic transcription, directly influencing mitotic progression (Dey *et al.*, 2009). It also recruits the positive transcription elongation factor complex (P-TEFb) to mitotic chromosomes, increasing the expression of growth-promoting genes (Yang *et al.*, 2005). The cyclin-dependent kinase 9 (Cdk9), which is part of the P-TEFb complex and activates transcription elongation through phosphorylation of RNA polymerase II, is already a validated target for a subset of malignancies, with its inhibitor flavopiridol undergoing clinical trials (Lolli, 2009, 2010). Finally, BRD4 is fused with NUT (nuclear protein in testis) as a consequence of a chromosomal translocation in the aggressive NUT midline carcinoma (French *et al.*, 2001, 2003) and the BET–BRD inhibitor I-BET762 has recently entered clinical trials for this pathology (ClinicalTrials.gov identifier NCT01587703). Anti-inflammatory effects in mice have also been reported for this inhibitor (Nicodeme *et al.*, 2010). The structurally related triazolodiazepine compounds I-BET762 and (+)-JQ1 (Filippakopoulos *et al.*, 2010) are the most potent BET–BRD inhibitors developed to date. Additional scaffolds (3,5-dimethylisoxazole and dihydroquinazolinone) have been shown to bind to BRD4 (Hewings *et al.*, 2011; Dawson *et al.*, 2011; Chung *et al.*, 2012; Fish *et al.*, 2012). One of these, I-BET151, induced cell-cycle arrest and apoptosis in mixed-lineage leukaemia (MLL) cells and also shows encouraging results in mouse models of MLL (Dawson *et al.*, 2011). The fragment-based drug-discovery approach is at present widely used for the development of new BRD4 inhibitors, with the most recent articles being published during the revision process of the

Table 1
Data-collection and refinement statistics.

N-BRD4 complexed with	*N*-Methyltrimethylacetamide	Pyrrolidinone	DMSO
Data collection			
Space group	$P2_12_12_1$	$P2_12_12_1$	$P2_12_12_1$
Unit-cell parameters (Å)	a = 37.20, b = 44.13, c = 77.96	a = 37.31, b = 44.40, c = 78.16	a = 37.18, b = 44.12, c = 77.96
X-ray source	ID23-1, ESRF	XRD1, Elettra	XRD1, Elettra
Wavelength (Å)	0.9724	1.200	1.200
Resolution (Å)	44.13–1.25 (1.32–1.25)	44.40–1.50 (1.58–1.50)	38.98–1.40 (1.48–1.40)
R_{merge} (%)	9.6 (49.6)	7.6 (37.3)	7.2 (46.8)
R_{meas} (%)	11.0 (57.5)	9.2 (46.0)	8.6 (58.5)
$R_{p.i.m.}$ (%)	5.3 (28.5)	5.1 (26.5)	4.6 (34.3)
$\langle I/\sigma(I)\rangle$	8.9 (2.8)	7.9 (2.1)	9.5 (2.0)
Completeness (%)	99.1 (96.7)	99.3 (98.8)	98.8 (97.3)
Multiplicity	4.3 (3.7)	2.9 (2.7)	3.1 (2.4)
Refinement			
Resolution (Å)	38.98–1.25	39.08–1.50	39.00–1.40
R_{work}/R_{free} (%)	14.9/16.7	16.9/19.4	15.9/19.1
No. of atoms			
Total	1357	1268	1321
Protein	1149	1089	1140
Ligand	8 + 4	6	4
Water	172	153	157
Ethylene glycol	24	20	20
B factors (Å^2)			
B_{Wilson}	8.4	11.6	8.9
Overall	11.0	13.7	10.9
Protein	9.5	12.5	9.5
Ligand	9.5	15.6	9.9
Water	20.1	21.5	19.8
Ethylene glycol	18.5	20.4	20.7
R.m.s. deviations			
Bond lengths (Å)	0.013	0.012	0.012
Bond angles (°)	1.7	1.5	1.5
Ramachandran plot, residues in (%)			
Favoured region	99.2	99.2	99.2
Allowed region	0.8	0.8	0.8
Outlier region	0	0	0
PDB entry	4ioo	4ioq	4ior

present manuscript (Chung *et al.*, 2012; Fish *et al.*, 2012; Zhao *et al.*, 2013). Here, we characterize the interference of DMSO, the most common solubilizing agent used for fragment libraries, with this approach, showing that its use could reduce the hit ratio of fragment libraries by a significant fraction.

We also show that different fragments can reproduce the different binding modes explored by bromodomains for recognition of variously modified substrates (*i.e.* mono-acetylated and diacetylated peptides).

2. Experimental procedures

The expression vector for the N-terminal bromodomain of BRD4 (N-BRD4) was obtained from the Structural Genomics Consortium, Oxford, England. Purified protein was obtained as described previously (Filippakopoulos *et al.*, 2010). Briefly, N-BRD4 expression in *Escherichia coli* BL21 cells was induced with 1 m*M* IPTG for 4 h at 291 K. The clarified lysate was passed through a DEAE column in the presence of 0.5 *M* NaCl and the unbound fraction containing the protein of interest was loaded onto a HisTrap column (GE Healthcare). Elution was performed using a step gradient of imidazole. The buffer was exchanged and

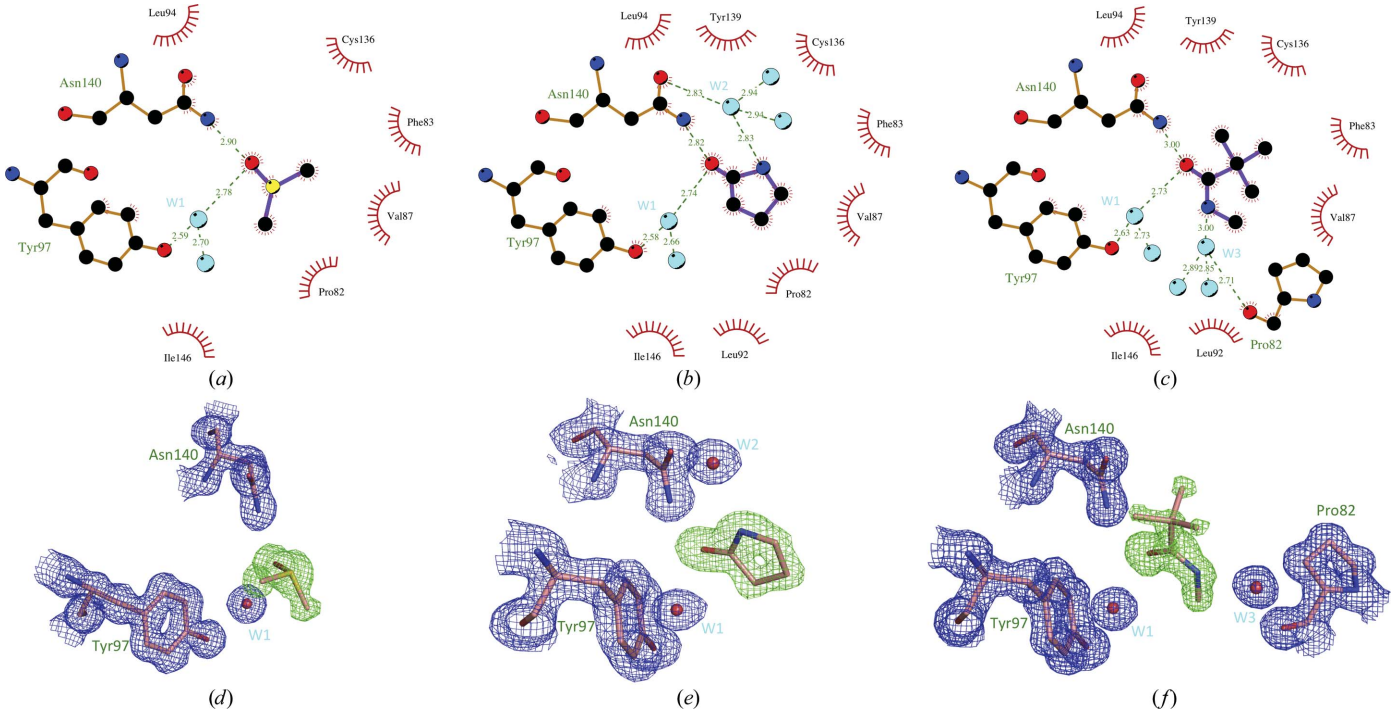

Figure 1
(*a*)–(*c*) N-BRD4–ligand interactions: (*a*) DMSO, (*b*) pyrrolidinone, (*c*) *N*-methyltrimethylacetamide. Hydrogen bonds are indicated by dashed lines, while hydrophobic contacts are represented by an arc with spokes radiating towards the ligand atoms that they contact. The contacted atoms are shown with spokes radiating back (prepared with *LigPlot*$^+$; Laskowski & Swindells, 2011). (*d*)–(*f*) Electron densities in the N-BRD4 K_{ac}-binding site: (*d*) DMSO, (*e*) pyrrolidinone, (*f*) *N*-methyltrimethylacetamide. Fragments are shown with corresponding simulated-annealing OMIT maps contoured at 3σ. $2F_o - F_c$ maps contoured at 1σ are shown for residues and water molecules involved in polar interactions with the fragments (prepared with *PyMOL*; http://www.pymol.org/).

the hexahistidine tag was removed with TEV protease. N-BRD4 was further purified on a Superdex 75 column (GE Healthcare) and was concentrated to 10 mg ml^{-1}.

N-BRD4 crystals were obtained at 277 K in sitting nanodrops using reservoir solutions consisting of 16% PEG 3350 and 20% ethylene glycol in the pH range 6.5–8.5. Small molecules purchased from Sigma–Aldrich were soaked at the following concentrations: 1% DMSO, 50 m*M* pyrrolidinone and 5 m*M* *N*-methyltrimethylacetamide in the presence of 1% DMSO. Crystals were cryoprotected by raising the PEG 3350 concentration to 20% and maintaining the ethylene glycol concentration at 20% in the soaking solutions. Soaking and cryoprotection were then performed simultaneously, adding the appropriate solution to the crystallization drop. After 2 h, the crystals were transferred into liquid nitrogen.

Diffraction data were collected at 100 K at the XRD1 and ID23-1 beamlines at Elettra, Trieste, Italy and the ESRF, Grenoble, France, respectively, and were integrated with *XDS* (Kabsch, 2010) before reduction and scaling with *SCALA* (Collaborative Computational Project, Number 4, 1994; Evans, 2006; Winn *et al.*, 2011). Molecular replacement was performed with *Phaser* (McCoy *et al.*, 2007) using the apo N-BRD4 structure (PDB entry 2oss; Filippakopoulos, Picaud, Mangos *et al.*, 2012) as a model. Models were inspected and modified with *Coot* (Emsley *et al.*, 2010) and were refined anisotropically with *REFMAC*5 (Murshudov *et al.*, 2011; Winn *et al.*, 2011). Water molecules were added with *PHENIX* (Adams *et al.*, 2010), which was also used for occupancy refinement of *N*-methyltrimethylacetamide and DMSO. The *PRODRG* server (Schüttelkopf & van Aalten, 2004) was used to obtain PDB and CIF files for the small molecules, which were manually placed in positive electron density using *Coot*. Anisotropic refinement was also applied to the ligands. Structures and structure-factor amplitudes have been deposited in the PDB (http://www.pdb.org/) as entries 4ioo, 4ioq and 4ior.

3. Results and discussion

Three structures of the first bromodomain of BRD4 (N-BRD4) are reported which have been solved to high resolution in complex with small molecules mimicking acetylated lysines (Table 1). The smallest of these, DMSO, was observed to interfere with the BRD solution assay for binding of histone peptides (Philpott *et al.*, 2011) and we first verified its binding to the N-BRD4 acetylated lysine-binding pocket by solving the structure of their complex. Subsequently, we investigated the possible interference of DMSO with the fragment-based approach for BRD4 drug discovery. In order to verify the effect of DMSO on soaking low-molecular-weight fragments in N-BRD4, we selected pyrrolidinone and *N*-methyltrimethylacetamide as test molecules. Pyrrolidinone was selected as a very low affinity fragment by removing part of the BRD-interacting region from *N*-methylpyrrolidinone (Filippakopoulos, Picaud, Mangos *et al.*, 2012; Chung *et al.*, 2012). *N*-Methyltrimethylacetamide was chosen as a better ligand starting from the observed interaction of *N*-methylacetamide with the GCN5 bromodomain (Hudson *et al.*, 2000). All three fragments are found in the acetylated lysine-binding pocket of N-BRD4, which is almost identical in the three structures.

DMSO only shows a single anchoring point (Figs. 1*a* and 1*d*): the hydrogen bonds to the side-chain amide N atom of Asn140 and to a conserved water molecule (W1, hydrogen bonding to Tyr97) observed in various structures of N-BRD4 in complex with K_{ac}-containing peptides (PDB entries 3uw9, 3uvw, 3uvy and 3uvx; Filippakopoulos, Picaud, Mangos *et al.*, 2012) or with different inhibitors and fragments. The hydrogen bond to Asn140 (2.90 Å) is shorter than those formed by K_{ac}-containing peptides or by the triazole and isoxazole moieties of BRD4 inhibitors (PDB entries 2yel, 3mxf, 3p5o, 3svf, 3svg, 3u5j, 3zyu and 4f3i; Filippakopoulos *et al.*, 2010; Nicodeme *et al.*, 2010; Hewings *et al.*, 2011; Chung *et al.*, 2011; Dawson *et al.*, 2011; Filippakopoulos, Picaud, Fedorov *et al.*, 2012; Zhang *et al.*, 2012). During the writing of this manuscript, various structures of N-BRD4 in complex with dihydroquinazolinone compounds have been deposited, with the cyclic urea carbonyl approaching Asn140 similarly to DMSO (PDB entries 4e96, 4hbw, 4hby and 4hbx; Fish *et al.*, 2012). With respect to the apo structure (PDB entry 2oss; Filippakopoulos, Picaud, Mangos *et al.*, 2012), DMSO displaces a single water molecule (that interacting with Asn140) and induces Ile146 to switch to a different conformer as observed in the ligand-bound N-BRD4 structures (except for the structure in complex with histone H4 Lys5–Lys8 diacetylated peptide; PDB entry 3uvw). Additional contacts involve Pro82, Phe83, Val87, Leu94, Tyr97 and Cys136. This structure was obtained by soaking N-BRD4 crystals with 1% DMSO, indicating that this solvent should be avoided when searching for additional low-affinity fragments that interact with the K_{ac}-binding site of BRDs. This is further described below in the structure of N-BRD4 in complex with *N*-methyltrimethylacetamide. The structure of the CREBBP bromodomain in complex with DMSO (PDB entry 3p1e; Structural Genomics Consortium, unpublished work) was solved to 1.8 Å resolution with two molecules per asymmetric unit and with slightly different orientations reported for the DMSO molecules in the two chains (mean displacement of 0.85 Å). In the complex with N-BRD4 at 1.4 Å resolution, DMSO is oriented similarly to as observed for chain *B* of PDB entry 3p1e.

All of the interactions described above are retained in the other two structures reported here. The pyrrolidinone molecule has an additional anchoring point *via* a water-bridged (W2) hydrogen bond between the N atom and the side-chain amide carbonyl of Asn140 (also present in the structure of N-BRD4 in complex with

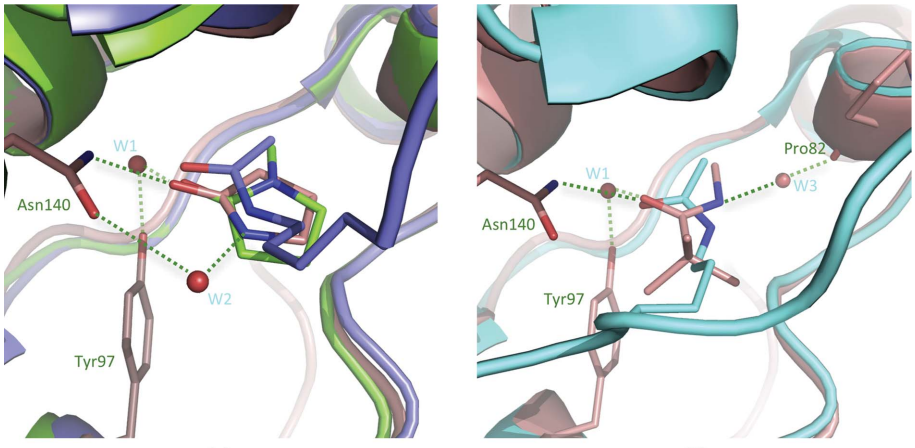

(*a*) (*b*)

Figure 2
(*a*) Comparison of the binding modes of pyrrolidinone (to N-BRD4; salmon) and *N*-methylpyrrolidinone (to N-BRD2; PDB entry 4a9f; green). $K8_{ac}$ in the histone H4 Lys8–Lys12 diacetylated peptide (PDB entry 3uw9; violet) binds to N-BRD4 similarly to pyrrolidinone. (*b*) *N*-Methyltrimethylacetamide binds to N-BRD4 similarly to $K16_{ac}$ in the histone H4 Lys16–Lys20 diacetylated peptide (PDB entry 3uvy; cyan).

6-bromo-3-methyl-3,4-dihydroquinazolin-2-one; PDB entry 4hbv; Fish *et al.*, 2012) and additionally contacts Leu92 and Tyr139 (Figs. 1*b* and 1*e*). It closely resembles the spatial organization of $K8_{ac}$ in the histone H4 Lys8–Lys12 diacetylated peptide bound to N-BRD4 (Fig. 2*a*); N-BRD4 does not contact $K12_{ac}$ and this structure represents the N-BRD4 monoacetylated recognition mode (PDB entry 3uw9; Filippakopoulos, Picaud, Mangos *et al.*, 2012). The structures of two different BRDs (the single bromodomain of BRD1 and the first bromodomain of BRD2) in complex with *N*-methylpyrrolidinone are available (PDB entries 3rcw and 4a9f; Filippakopoulos, Picaud, Mangos *et al.*, 2012; Chung *et al.*, 2012). In both cases the pyrrolidinone ring is tilted 180° with respect to that observed in our structure (Fig. 2*a*). The additional methyl group impedes the hydrogen bond to W2 while more deeply exploring the K_{ac}-binding site.

Similarly, in the last structure presented here, the complex with *N*-methyltrimethylacetamide, the amide group is tilted with respect to the pyrrolidinone molecule. As a consequence, the acetamide N atom anchors to a different point, with a water-bridged (W3) hydrogen bond to the backbone carbonyl of Pro82 (Figs. 1*c* and 1*f*). Interestingly, this interaction is also present in the structures of N-BRD4 in complex with histone H4 Lys5–Lys8, Lys12–Lys16 and Lys16–Lys20 diacetylated peptides (Fig. 2*b*). In these structures, the two acetylated lysines bind simultaneously and with identical conformations to N-BRD4, representing the diacetylated recognition mode (PDB entries 3uvw, 3uvy and 3uvx; Filippakopoulos, Picaud, Mangos *et al.*, 2012). In comparison with the pyrrolidinone molecule, *N*-methyltrimethylacetamide also shows extended van der Waals contacts with Tyr139. This complex was obtained by soaking N-BRD4 crystals with 5 m*M* *N*-methyltrimethylacetamide in the presence of 1% DMSO. Both molecules are present in the K_{ac}-binding site, with refined occupancies of 0.65 and 0.35, respectively.

The structure of N-BRD4 in complex with pyrrolidinone was obtained by soaking the fragment at a concentration of 50 m*M* in the absence of DMSO, while the lower concentration of 5 m*M* only led to partial occupancy of the N-BRD4 pocket. When 1% DMSO was used in conjunction with 5 m*M* pyrrolidinone, only DMSO was visible in the electron density. As expected, pyrrolidinone has a lower affinity for N-BRD4 with respect to *N*-methyltrimethylacetamide; a pyrrolidinone:DMSO concentration ratio of 1:28 makes the pyrrolidinone–BRD4 interaction undetectable.

Fragments considered useful as starting points for the development of hit compounds bind their targets with affinities in the high micromolar to low millimolar range. DMSO is generally used as a solubilizing agent at a concentration 10–100 times greater than that of the tested fragments. Our data indicate that, at least in the case of N-BRD4, this would result in a number of false negatives, with the binding of many if not all fragments with millimolar affinities being undetectable in the presence of DMSO.

The structures presented here also highlight the possibility of using different acetylated lysine-mimicking molecules as tools to explore the different target-recognition modes exploited by BRDs.

We are grateful to Professor Stefan Knapp (Structural Genomics Consortium, Oxford) for providing us with the expression vector for N-BRD4 and to the staff of the ID23-1 and XRD1 beamlines at ESRF, Grenoble, France and Elettra, Trieste, Italy, respectively. This work was supported by a FEBS Distinguished Young Investigator Award granted to GL.

References

Adams, P. D. *et al.* (2010). *Acta Cryst.* D**66**, 213–221.
Chung, C.-W. *et al.* (2011). *J. Med. Chem.* **54**, 3827–3838.
Chung, C.-W., Dean, A. W., Woolven, J. M. & Bamborough, P. (2012). *J. Med. Chem.* **55**, 576–586.
Collaborative Computational Project, Number 4 (1994). *Acta Cryst.* D**50**, 760–763.
Dawson, M. A. *et al.* (2011). *Nature (London)*, **478**, 529–533.
Dey, A., Nishiyama, A., Karpova, T., McNally, J. & Ozato, K. (2009). *Mol. Biol. Cell*, **20**, 4899–4909.
Emsley, P., Lohkamp, B., Scott, W. G. & Cowtan, K. (2010). *Acta Cryst.* D**66**, 486–501.
Evans, P. (2006). *Acta Cryst.* D**62**, 72–82.
Filippakopoulos, P. *et al.* (2010). *Nature (London)*, **468**, 1067–1073.
Filippakopoulos, P., Picaud, S., Fedorov, O., Keller, M., Wrobel, M., Morgenstern, O., Bracher, F. & Knapp, S. (2012). *Bioorg. Med. Chem.* **20**, 1878–1886.
Filippakopoulos, P., Picaud, S., Mangos, M., Keates, T., Lambert, J. P., Barsyte-Lovejoy, D., Felletar, I., Volkmer, R., Müller, S., Pawson, T., Gingras, A. C., Arrowsmith, C. H. & Knapp, S. (2012). *Cell*, **149**, 214–231.
Fish, P. V. *et al.* (2012). *J. Med. Chem.* **55**, 9831–9837.
French, C. A., Miyoshi, I., Aster, J. C., Kubonishi, I., Kroll, T. G., Dal Cin, P., Vargas, S. O., Perez-Atayde, A. R. & Fletcher, J. A. (2001). *Am. J. Pathol.* **159**, 1987–1992.
French, C. A., Miyoshi, I., Kubonishi, I., Grier, H. E., Perez-Atayde, A. R. & Fletcher, J. A. (2003). *Cancer Res.* **63**, 304–307.
Hewings, D. S., Wang, M., Philpott, M., Fedorov, O., Uttarkar, S., Filippakopoulos, P., Picaud, S., Vuppusetty, C., Marsden, B., Knapp, S., Conway, S. J. & Heightman, T. D. (2011). *J. Med. Chem.* **54**, 6761–6770.
Hudson, B. P., Martinez-Yamout, M. A., Dyson, H. J. & Wright, P. E. (2000). *J. Mol. Biol.* **304**, 355–370.
Kabsch, W. (2010). *Acta Cryst.* D**66**, 125–132.
Laskowski, R. A. & Swindells, M. B. (2011). *J. Chem. Inf. Model.* **51**, 2778–2786.
Lolli, G. (2009). *Nucleic Acids Res.* **37**, 1260–1268.
Lolli, G. (2010). *Cell Cycle*, **9**, 1551–1561.
McCoy, A. J., Grosse-Kunstleve, R. W., Adams, P. D., Winn, M. D., Storoni, L. C. & Read, R. J. (2007). *J. Appl. Cryst.* **40**, 658–674.
Murshudov, G. N., Skubák, P., Lebedev, A. A., Pannu, N. S., Steiner, R. A., Nicholls, R. A., Winn, M. D., Long, F. & Vagin, A. A. (2011). *Acta Cryst.* D**67**, 355–367.
Nicodeme, E. *et al.* (2010). *Nature (London)*, **468**, 1119–1123.
Owen, D. J., Ornaghi, P., Yang, J.-C., Lowe, N., Evans, P. R., Ballario, P., Neuhaus, D., Filetici, P. & Travers, A. A. (2000). *EMBO J.* **19**, 6141–6149.
Philpott, M., Yang, J., Tumber, T., Fedorov, O., Uttarkar, S., Filippakopoulos, P., Picaud, S., Keates, T., Felletar, I., Ciulli, A., Knapp, S. & Heightman, T. D. (2011). *Mol. Biosyst.* **7**, 2899–2908.
Schüttelkopf, A. W. & van Aalten, D. M. F. (2004). *Acta Cryst.* D**60**, 1355–1363.
Winn, M. D. *et al.* (2011). *Acta Cryst.* D**67**, 235–242.
Yang, Z., Yik, J. H. N., Chen, R., He, N., Jang, M. K., Ozato, K. & Zhou, Q. (2005). *Mol. Cell*, **19**, 535–545.
Zhang, G., Liu, R., Zhong, Y., Plotnikov, A. N., Zhang, W., Zeng, L., Rusinova, E., Gerona-Nevarro, G., Moshkina, N., Joshua, J., Chuang, P. Y., Ohlmeyer, M., He, J. C. & Zhou, M.-M. (2012). *J. Biol. Chem.* **287**, 28840–28851.
Zhao, L., Cao, D., Chen, T., Wang, Y., Miao, Z., Xu, Y., Chen, W., Wang, X., Li, Y., Du, Z., Xiong, B., Li, J., Xu, C., Zhang, N., He, J. & Shen, J. (2013). *J. Med. Chem.* **56**, 3833–3851.